

The Doppler effect on indirect detection of dark matter

Devon Powell,^{1,2,*} Ranjan Laha,^{1,2,†} and Tom Abel^{1,2}

¹*Kavli Institute for Particle Astrophysics and Cosmology (KIPAC),
Department of Physics, Stanford University, Stanford, CA 94305, USA*
²*SLAC National Accelerator Laboratory, Menlo Park, CA 94025, USA*

(Dated: September 16, 2016)

[1]

I Introduction: The search for the particle properties of dark matter is one of the most important research avenues [2–4]. The “weak” interactions experienced by the dark matter particle complicates these searches. Despite decades of multi-pronged searches, we have not yet identified the dark matter particle [5]. One of the most important ways to search for dark matter particles is indirect detection [6].

Many anomalous signals have been interpreted as arising from dark matter interactions [7–15]. Astrophysical sources such as pulsars or atomic lines are diverse enough to mimic a dark matter signal [16–21]. The separation of signal and background is difficult since one needs to model these in the same data set. Taking lessons from all these misadventures, it is prudent to ask for new methods to cleanly separate the signal and background. This is especially important since there are many viable dark matter candidates which can only be detected via astrophysical observations.

Distinct kinematic signatures arising from dark matter annihilation or decay are used to separate the dark matter signal from background. These signatures include monochromatic photons arising from dark matter annihilation or decay. Past experiences have shown that it is not reliable to only depend on this kinematic end point signature for the identification of a dark matter signal. Additional checks are required to completely confirm a dark matter signal.

In order to better characterize a dark matter signal, Ref. [1] utilized the superb energy resolution, $\sim \mathcal{O}(0.1\%)$, of Hitomi (previously known as Astro-H) to find a new signature — dark matter velocity spectroscopy. Solar motion around the Galaxy produces a distinct longitudinal dependence in the dark matter signal, a signature of Doppler effect. This new signature is model independent and applicable to any dark matter signal containing a sharp feature. It is unlikely that baryonic phenomenon can produce such a distinct signature [1].

Given the importance of dark matter particle searches, it is important to characterize any new model independent signature in detail. While Hitomi had a narrow field of view, it is important to confirm if dark matter velocity spectroscopy can also be performed by a high energy

resolution instrument with a wide field of view. We perform such a study in this work using dark matter only simulations from Ref. [22]. As an example of the dark matter signal, we consider the 3.5 keV line [13, 14]. The status of the 3.5 keV line is controversial [23–32]. The malfunctioning of the Hitomi satellite did not permit an observation to conclusively test this signal. We use future Micro-X observations [33] to demonstrate our technique. It is expected that Micro-X will have an energy resolution of 3 eV at 3.5 keV [33], a high enough energy resolution to permit dark matter velocity spectroscopy [1]. We emphasize that we are using this 3.5 keV signal as a proxy, and that the underlying physics of dark matter velocity spectroscopy is model independent.

There have been many works in which velocity spectroscopy was used to understand baryonic astrophysical emission [34–37]. Ref. [1] first applied this technique analytically to dark matter. In this work, we analyze for the *first* time dark matter velocity spectroscopy using realistic dark matter simulations

Any telescope with $\mathcal{O}(0.1\%)$ energy resolution can perform dark matter velocity spectroscopy. An improvement in the energy resolution is the natural step in the evolution of telescope instrumentation. This improvement will help in disentangling the dark matter signal from background, and improve our knowledge of the astronomical sources. For certain wavelengths, it is already known how to build a detector with $\mathcal{O}(0.1\%)$ energy resolution, such as INTEGRAL/ SPI [38] and Hitomi. Near future instruments like Micro-X [33] and ATHENA X-IFU [39] will also have $\mathcal{O}(0.1\%)$ energy resolution.

II Methods:

A Theory: In this subsection, we outline the theoretical insights leading to dark matter velocity spectroscopy [1]. The discussion is tailored for a wide field of view instrument like Micro-X.

For instruments with an energy resolution, $\Delta E/E \gg \mathcal{O}(0.1\%)$, the differential flux of photons originating from dark matter decay in the Milky Way halo is given by [33]:

$$\frac{d^2 \mathcal{F}}{d\Omega dE} = \frac{\Gamma}{4\pi m_s} \frac{dN(E)}{dE} \int_0^{s_{\max}} ds \rho[r(s, \Omega)]. \quad (1)$$

Here \mathcal{F} denotes the flux in $\text{cm}^{-2} \text{s}^{-1}$, Ω denotes the solid angle in sr, E denotes the energy of the photon in keV,

*dmpowell@stanford.edu

†rlaha@stanford.edu

and Γ denotes the decay rate (in s^{-1}) of the dark matter particle of mass m_s (in keV). The dark matter density (in keV cm^{-3}) profile is denoted by $\rho(r)$, and the photon spectrum (in keV^{-1}) is denoted by $dN(E)/dE$. The line of sight distance, s , varies from 0 to s_{max} , where the maximum value of the line of sight distance, s_{max} , corresponds to the virial radius of the Milky Way halo.

In this work, we are concerned with sterile neutrino, ν_s , decay to an active neutrino, ν_a , and a photon, γ : $\nu_s \rightarrow \nu_a + \gamma$. This implies that the photon energy $E = m_s/2$. We concentrate on the detection of photons in this work, as the constraint from the detection of active neutrino is weak.

Observation by a telescope with $\sim \mathcal{O}(0.1\%)$ energy resolution modifies this above expression, Eqn. 1, in two important and distinct ways. First, the photon line is broadened due to the velocity dispersion of the dark matter particles in the Milky Way halo. Second, the energy of the photon is shifted depending on the Doppler shifting of the line.

We take into account the broadening of the line by convolving the $dN(E)/dE$ by a Gaussian of width $\sigma_E = (E/c)\sigma_{v_{\text{LOS}}}$ [1]. Here $\sigma_{v_{\text{LOS}}}$ corresponds to the line of sight velocity dispersion of dark matter. The form of Gaussian arises since we consider a Maxwellian dark matter velocity distribution. The line shape will change if we consider dark matter velocity distribution favored by recent hydrodynamical simulations [40–42], but we ignore the difference in this work.

The broadened line shape can be written as

$$\frac{d\tilde{N}(E, r[s, \Omega])}{dE} = \int dE' \delta\left(E' - \frac{m_s}{2}\right) \times G(E - E', \sigma_{E'}(r[s, \Omega])), \quad (2)$$

where the convolution function is a Gaussian as mentioned above. The width of the Gaussian, $\sigma_E(r[s, \Omega])$ is calculated following Ref. [1].

Since the solar velocity is nonrelativistic, we can use the usual formula for Doppler shift: $\Delta E/E = -v_{\text{LOS}}/c$. Following Ref. [1], we define $v_{\text{LOS}} = (\langle \mathbf{v}_\chi \rangle - \mathbf{v}_\odot) \cdot \hat{r}_{\text{LOS}}$. We assume $\langle \mathbf{v}_\chi \rangle \approx 0$, and $v_\odot = 220 \text{ km s}^{-1}$. In the coordinate system where the x-axis is towards the Galactic Center, the direction of the Galactic rotation is in the y direction, and the z-axis is the normal to the Galactic plane, we have $\mathbf{v}_\odot = v_\odot \hat{y}$. In this reference frame, $\mathbf{v}_\odot \cdot \hat{r}_{\text{LOS}} = v_\odot y/|r_{\text{LOS}}|$. In terms of the Galactic longitude, ℓ , and Galactic latitude, b , we have $y = r_{\text{LOS}} \sin \ell \cos b$. From this, we have $\Delta E/E = v_\odot (\sin \ell) (\cos b)$.

Taking these two effects into account, we can rewrite Eqn. 1 as

$$\frac{d^2 \mathcal{F}(\ell, b)}{d\Omega dE} = \frac{\Gamma}{4\pi m_s} \int_0^{s_{\text{max}}} ds \rho[r(s, \Omega)] \times \frac{d\tilde{N}(E - \Delta E(\ell, b), r(s, \Omega))}{dE}. \quad (3)$$

An important difference in the narrow field of view and wide field of view instruments is encapsulated in

$\Delta E(\ell, b)$. For Hitomi with a field of view of 9 arcmin^2 , the maximum value of the line intensity approximately occurs at the (ℓ, b) corresponding to the center of the field of view. This is not true for a wide field of view instrument like Micro-X (20° radius field of view). The maximum value of the line intensity depends on the density profile as is evident from Eqn. 3.

The shift in the central value of the energy of the widened line is shown by the argument $E - \Delta E(\ell, b)$. Both the width of the line and the position of the central value of the line is determined by the position of the line and this is indicated by $r(s, \Omega)$ the argument of $d\tilde{N}/dE$.

B Simulations: Should we add a few sentences on why we are using a CDM simulations? One can take a simulation with the same parameters as 3.5 keV line but it does not make a big difference — see for e.g. [43]. We can also say that we are not really concentrating on 3.5 keV line but using it as a test model — something like that — We should add this clarification at the end of this subsection.

Numerical simulations take into account many different processes which participate in dark matter halo formation. Many signatures of these non linear processes are not taken into account in an analytical model of the dark matter halo. It is thus important to validate any new signature of dark matter by using realistic simulations of galaxy formation.

We evaluate the potential of dark matter velocity spectroscopy using dark-matter-only N-body simulations. We study a suite of Milky Way analogues run using the L-GADGET cosmology code (a descendant of GADGET-2 [44]). These are dark-matter-only zoom-in simulations run by Ref. [22] to study subhalo abundance. Their high resolution and multiple realizations makes them suitable for our purposes as well. Each halo has $\mathcal{O}(10^7)$ high-resolution particles with a particle mass $m_p = 4.0 \times 10^5 M_\odot$ and total mass $M_{\text{vir}} \simeq 1.2 \times 10^{12} M_\odot$ (masses in physical units). Do all halos have this mass? I am slightly unsure of how much details of the simulation we should give. We can simply refer the readers to the older papers. If we decide to give the details of the simulation, then we need to provide the cosmological parameters, and the softening length in addition to the particle mass that you mentioned.

Among the 46 halo realizations, we focus on one halo, Halo 374, (Figure 1) in detail. This is the most spherically-symmetric halo, with principal axis ratios $b/a = 0.86$ and $c/a = 0.73$. We choose this halo to facilitate the comparison of our results with a spherically symmetric generalized NFW profile of the halo. Dark-matter-only simulations produce triaxial halos, but recent hydrodynamical simulations have shown that the inclusion of baryons tend to sphericalize a halo [45–48].

Although hydrodynamical models are investigated by many groups, yet it is not known if all the baryonic processes are self consistently taken into account in these

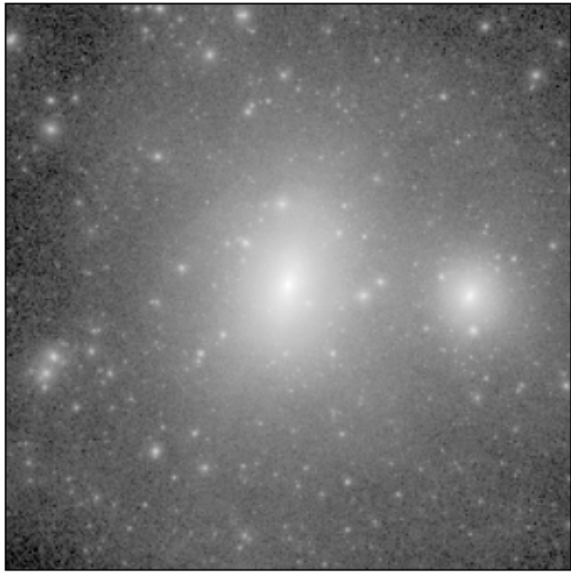


FIG. 1. Halo 374. *Need to write more in the caption. Especially what does the color scale indicate? People use the color scale to indicate the density squared or density. What have you taken? Since we are mainly focusing on decaying dark matter, it will be better to use the color scale to indicate density.*

simulations. To take into account these uncertainties, we will also show our results for halos which are less spherical compared to Halo 374. The statistical significance of the result depends on the triaxiality of the halo.

C Velocity spectroscopy using simulations: In order to generalize the analytical methods presented in Sec. II A to a simulation containing N-body particles, we simply convert the integration to a sum over the N-body particles. This is similar in spirit to the “sightline” method employed by [43] and the velocity distribution function sampling of [49]. We construct the full spectral intensity seen by the detector directly from the N-body particles, incorporating Doppler shift and velocity dispersion.

The dark matter density field, $\rho(\mathbf{x})$, in a position \mathbf{x} in an N-body simulation is effectively a sum of Dirac- δ functions:

$$\rho(\mathbf{x}) = \sum_p m_p \delta(\mathbf{x} - \mathbf{x}_p), \quad (4)$$

where \mathbf{x}_p and m_p are the position and mass of particle p .

The total flux can be found by integrating the differential flux in Eqn. 1 over the energy and solid angle. Implementing this in an N-body simulation implies a summation over all of the particles, p , within the field of view, Ω , and weighting by the inverse square of the scalar distance

to the observer, r_p^{-2} :

$$\mathcal{F} = \frac{\Gamma}{4\pi m_s} \sum_{p \in \Omega} \frac{m_p}{r_p^2}, \quad (5)$$

The differential flux in energy can also be calculated in a similar way:

$$\frac{d\mathcal{F}}{dE} = \frac{\Gamma}{4\pi m_s} \sum_{p \in \Omega} \frac{m_p}{r_p^2} \frac{dN[E(1 - v_p/c)]}{dE}, \quad (6)$$

where v_p is the velocity of particle p projected along the line of sight to the observer. By considering the LOS velocity of each particle independently, we automatically capture the spectral convolution introduced by the bulk velocity dispersion.

We focus here on the special case where dN/dE is a line due to sterile neutrino decay. The parameters of the sterile neutrino are those favored by the 3.5 keV line [13]. In this case, computing the observed spectrum is then as simple as building a flux-weighted histogram of the line-of-sight velocities for all particles in the sampling cone, though as we will see it is easier to forgo binning and compute the line width directly. See Figure 2 for an illustration. *I am not sure what you mean by the last sentence.*

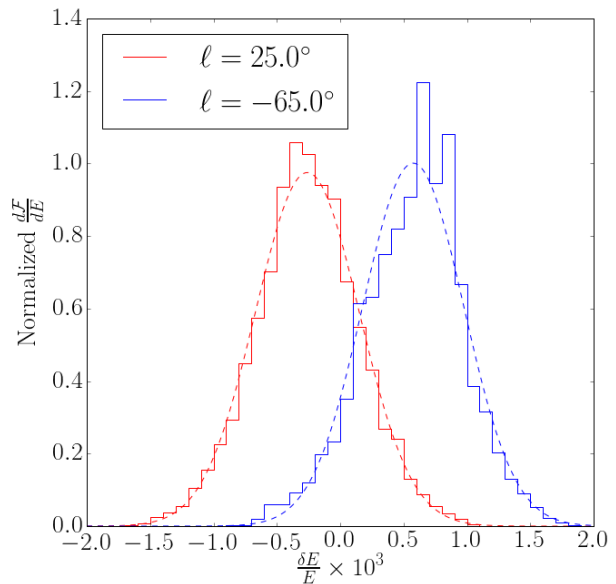


FIG. 2. We plot the normalized $d\mathcal{F}/dE$ versus the fractional shift in the energy $\delta E/E$ (the x-axis is multiplied by 1000 for clarity). The field of view is centered at $(\ell, b) = (25^\circ, 25^\circ)$, and $(-65^\circ, 25^\circ)$. The dashed line is a Gaussian model fit to the analytical calculation, whereas the histogram is calculated directly from the simulations.

The flux-weighted mean line-of-sight velocity for a field

of view is

$$\langle v \rangle = \frac{1}{\mathcal{F}} \frac{\Gamma}{4\pi m_s} \sum_{p \in \Omega} \frac{m_p}{r_p^2} v_p \quad (7)$$

For non relativistic velocities, the mean Doppler shift (the observed shift in the energy of the line) is $\langle \delta E \rangle = (E/c)\langle v \rangle$. We compute the width of the observed line σ_E directly by finding the flux-weighted variance of the line-of-sight velocities v_p :

$$\sigma_v^2 = \frac{1}{\mathcal{F}} \frac{\Gamma}{4\pi m_s} \sum_{p \in \Omega} \frac{m_p}{r_p^2} (v_p - \langle v \rangle)^2 \quad (8)$$

The width of the Doppler-broadened line is then $\sigma_E = (E/c)\sigma_v$.

We compare the line width and shift computed analytically and directly from simulations in Fig. 2 for two different field of views centered at $(\ell, b) = (25^\circ, 25^\circ)$ and $(-65^\circ, 25^\circ)$. The analytical computation is shown by dashed line, whereas the solid line shows the lines computed directly from the simulations. Good agreement is seen between these two different computations for this halo.

D Model observation by Micro-X: The instrument that we focus on in this work is Micro-X [33]. It is a direct successor to the XQC sounding rocket experiment [50–52]. We follow the parameters of the instrument near 3.5 keV as mentioned in [33]: field of view: 20° radius, effective area = 1 cm^2 , and an exposure time = 300 s.

To minimize contamination by the Galactic plane, we focus on field of views which are centered at $b = 25^\circ$ for various different Galactic longitudes, ℓ . This choice is a compromise between the decreasing signal strength away from the Galactic Center, and the more rapidly decreasing background away from the Galactic plane. A typical sterile neutrino decay flux at 3.5 keV from the Milky Way halo at $b = 25^\circ$ is $\mathcal{F} \sim 0.05 \text{ photons cm}^{-2} \text{ str}^{-1} \text{ s}^{-1}$ for a signal count $N_s \sim 3 - 12$ photons, depending on ℓ .

We model the background N_b using the cosmic X-ray background model of [53]. The use of an alternative

model [54] for the cosmic X-ray background does not alter our conclusions. For both of these models, we obtain $N_b \sim 1$ photon per pointing.

We adopt the same model as [1] when treating the photon counting statistics in the energy of a decay line. The uncertainty in the energy of the line centroid is given by

$$\sigma_{\text{cent}} = (\sigma_E^2 + \sigma_{\text{inst}}^2)^{1/2} C(N_b/N_s) N_s^{-1/2} \quad (9)$$

where σ_{inst} is the instrumental uncertainty in energy (corresponding to the spectral resolution), N_s and N_b are the number of signal and background photons, respectively, and $C(R) = \sqrt{1 + 4R}$ is factor given by the Cramer-Rao bound for the given signal-to-background ratio.

Our figure of merit for a detection of a Doppler-shifted line is the probability that the data exclude zero shifting. In other words, we consider the energy shift of the line centroid away from $\delta E/E = 0$ in units of σ_{cent} . This most strongly depends on N_s , which we discuss in the results section. **I think we need to change the last two paragraphs — it will depend on the statistical analysis that you are doing now.**

III Results:

IV Conclusions: Very often in the past, anomalous astrophysical signals have been interpreted as the signature of dark matter. However, none of these extraordinary claims survived the scrutiny of extraordinary evidence. All of these false alarms raises an important question: can we design a new test to confirm the dark matter origin of an anomalous astrophysical signal? The answer is yes, and Ref. [1] showed that telescopes with $\mathcal{O}(0.1\%)$ energy resolution can utilize the Doppler effect of a sharp signal arising from dark matter interactions to perform dark matter velocity spectroscopy.

We look into this issue in detail in this work.

Acknowledgments: Mark Lovell, Yao-Yuan Mao, Chris Davis.

-
- [1] E. G. Speckhard, K. C. Y. Ng, J. F. Beacom, and R. Laha, *Physical Review Letters* **116**, 031301 (2016), [arXiv:1507.04744](#).
 - [2] G. Jungman, M. Kamionkowski, and K. Griest, *Phys. Rept.* **267**, 195 (1996), [arXiv:hep-ph/9506380 \[hep-ph\]](#).
 - [3] G. Bertone, D. Hooper, and J. Silk, *Phys. Rept.* **405**, 279 (2005), [arXiv:hep-ph/0404175 \[hep-ph\]](#).
 - [4] L. E. Strigari, *Phys. Rept.* **531**, 1 (2013), [arXiv:1211.7090 \[astro-ph.CO\]](#).
 - [5] G. Bertone and D. Hooper, Submitted to: Rev. Mod. Phys.(2016), [arXiv:1605.04909 \[astro-ph.CO\]](#).
 - [6] M. Klasen, M. Pohl, and G. Sigl, *Prog. Part. Nucl. Phys.* **85**, 1 (2015), [arXiv:1507.03800 \[hep-ph\]](#).
 - [7] M. Loewenstein and A. Kusenko, *Astrophys. J.* **714**, 652 (2010), [arXiv:0912.0552 \[astro-ph.HE\]](#).
 - [8] D. A. Prokhorov and J. Silk, *Astrophys. J.* **725**, L131 (2010), [arXiv:1001.0215 \[astro-ph.HE\]](#).
 - [9] C. Weniger, *JCAP* **1208**, 007 (2012), [arXiv:1204.2797 \[hep-ph\]](#).
 - [10] K. N. Abazajian, N. Canac, S. Horiuchi, M. Kaplinghat, and A. Kwa, *JCAP* **1507**, 013 (2015), [arXiv:1410.6168 \[astro-ph.HE\]](#).

- [11] S. K. Lee, M. Lisanti, B. R. Safdi, T. R. Slatyer, and W. Xue, *Phys. Rev. Lett.* **116**, 051103 (2016), [arXiv:1506.05124 \[astro-ph.HE\]](#).
- [12] R. Bartels, S. Krishnamurthy, and C. Weniger, *Phys. Rev. Lett.* **116**, 051102 (2016), [arXiv:1506.05104 \[astro-ph.HE\]](#).
- [13] E. Bulbul, M. Markevitch, A. Foster, R. K. Smith, M. Loewenstein, and S. W. Randall, *Astrophys. J.* **789**, 13 (2014), [arXiv:1402.2301 \[astro-ph.CO\]](#).
- [14] A. Boyarsky, O. Ruchayskiy, D. Iakubovskiy, and J. Franse, *Phys. Rev. Lett.* **113**, 251301 (2014), [arXiv:1402.4119 \[astro-ph.CO\]](#).
- [15] O. Urban, N. Werner, S. W. Allen, A. Simionescu, J. S. Kaastra, and L. E. Strigari, *Mon. Not. Roy. Astron. Soc.* **451**, 2447 (2015), [arXiv:1411.0050 \[astro-ph.CO\]](#).
- [16] R. M. O’Leary, M. D. Kistler, M. Kerr, and J. Dexter(2015), [arXiv:1504.02477 \[astro-ph.HE\]](#).
- [17] T. D. Brandt and B. Kocsis, *Astrophys. J.* **812**, 15 (2015), [arXiv:1507.05616 \[astro-ph.HE\]](#).
- [18] R. M. O’Leary, M. D. Kistler, M. Kerr, and J. Dexter(2016), [arXiv:1601.05797 \[astro-ph.HE\]](#).
- [19] L. Gu, J. Kaastra, A. J. J. Raassen, P. D. Mullen, R. S. Cumbee, D. Lyons, and P. C. Stancil, *Astron. Astrophys.* **584**, L11 (2015), [arXiv:1511.06557 \[astro-ph.HE\]](#).
- [20] K. J. H. Phillips, B. Sylwester, and J. Sylwester, *Astrophys. J.* **809**, 50 (2015).
- [21] C. Shah, S. Dobrodey, S. Bernitt, R. Steinbrugge, J. R. C. Lopez-Urrutia, L. Gu, and J. Kaastra(2016), [arXiv:1608.04751 \[astro-ph.HE\]](#).
- [22] Y.-Y. Mao, M. Williamson, and R. H. Wechsler, *Astrophys. J.* **810**, 21 (2015), [arXiv:1503.02637](#).
- [23] D. Iakubovskiy(2015), [arXiv:1510.00358 \[astro-ph.HE\]](#).
- [24] T. E. Jeltema and S. Profumo, *Mon. Not. Roy. Astron. Soc.* **458**, 3592 (2016), [arXiv:1512.01239 \[astro-ph.HE\]](#).
- [25] O. Ruchayskiy, A. Boyarsky, D. Iakubovskiy, E. Bulbul, D. Eckert, J. Franse, D. Malyshev, M. Markevitch, and A. Neronov, *Mon. Not. Roy. Astron. Soc.* **460**, 1390 (2016), [arXiv:1512.07217 \[astro-ph.HE\]](#).
- [26] E. Bulbul, M. Markevitch, A. Foster, E. Miller, M. Bautz, M. Loewenstein, S. W. Randall, and R. K. Smith(2016), [arXiv:1605.02034 \[astro-ph.HE\]](#).
- [27] F. A. Aharonian *et al.* (Hitomi)(2016), [arXiv:1607.07420 \[astro-ph.HE\]](#).
- [28] F. Hofmann, J. S. Sanders, K. Nandra, N. Clerc, and M. Gaspari, *Astron. Astrophys.* **592**, A112 (2016), [arXiv:1606.04091 \[astro-ph.CO\]](#).
- [29] C. A. Argüelles, V. Brdar, and J. Kopp(2016), [arXiv:1605.00654 \[hep-ph\]](#).
- [30] J. P. Conlon, F. Day, N. Jennings, S. Krippendorf, and M. Rummel(2016), [arXiv:1608.01684 \[astro-ph.HE\]](#).
- [31] A. Neronov, D. Malyshev, and D. Eckert(2016), [arXiv:1607.07328 \[astro-ph.HE\]](#).
- [32] K. Perez, K. C. Y. Ng, J. F. Beacom, C. Hersh, S. Horiuchi, and R. Krivonos(2016), [arXiv:1609.00667 \[astro-ph.HE\]](#).
- [33] E. Figueroa-Feliciano *et al.* (XQC), *Astrophys. J.* **814**, 82 (2015), [arXiv:1506.05519 \[astro-ph.CO\]](#).
- [34] T. M. Dame, D. Hartmann, and P. Thaddeus, *Astrophys. J.* **547**, 792 (2001), [arXiv:astro-ph/0009217 \[astro-ph\]](#).
- [35] R. Diehl *et al.*, *Nature* **439**, 45 (2006), [arXiv:astro-ph/0601015 \[astro-ph\]](#).
- [36] P. M. W. Kalberla and L. Dedes, *Astron. Astrophys.* **487**, 951 (2008), [arXiv:0804.4831 \[astro-ph\]](#).
- [37] K. Kretschmer, R. Diehl, M. Krause, A. Burkert, K. Fierlinger, O. Gerhard, J. Greiner, and W. Wang, *Astron. Astrophys.* **559**, A99 (2013), [arXiv:1309.4980 \[astro-ph.HE\]](#).
- [38] D. Attie *et al.*, *Astronomy and Astrophysics* **411**, L71 (2003), [arXiv:astro-ph/0308504](#).
- [39] D. Barret *et al.*(2016), doi:\bibinfo{doi}{10.1117/12.2232432}, [arXiv:1608.08105 \[astro-ph.IM\]](#).
- [40] N. Bozorgnia, F. Calore, M. Schaller, M. Lovell, G. Bertone, C. S. Frenk, R. A. Crain, J. F. Navarro, J. Schaye, and T. Theuns, *JCAP* **1605**, 024 (2016), [arXiv:1601.04707 \[astro-ph.CO\]](#).
- [41] J. D. Sloane, M. R. Buckley, A. M. Brooks, and F. Governato(2016), [arXiv:1601.05402 \[astro-ph.GA\]](#).
- [42] C. Kelso, C. Savage, M. Valluri, K. Freese, G. S. Stinson, and J. Bailin(2016), [arXiv:1601.04725 \[astro-ph.GA\]](#).
- [43] M. R. Lovell, G. Bertone, A. Boyarsky, A. Jenkins, and O. Ruchayskiy, *Mon. Not. Roy. Astron. Soc.* **451**, 1573 (2015), [arXiv:1411.0311 \[astro-ph.CO\]](#).
- [44] V. Springel, *M.N.R.A.S.* **364**, 1105 (2005), [arXiv:astro-ph/0505010](#).
- [45] V. P. Debattista, B. Moore, T. R. Quinn, S. Kazantzidis, R. Maas, L. Mayer, J. Read, and J. Stadel, *Astrophys. J.* **681**, 1076 (2008), [arXiv:0707.0737 \[astro-ph\]](#).
- [46] S. E. Bryan, S. T. Kay, A. R. Duffy, J. Schaye, C. D. Vecchia, and C. M. Booth, *Mon. Not. Roy. Astron. Soc.* **429**, 3316 (2013), [arXiv:1207.4555 \[astro-ph.CO\]](#).
- [47] N. Bernal, J. E. Forero-Romero, R. Garani, and S. Palomares-Ruiz, *JCAP* **1409**, 004 (2014), [arXiv:1405.6240 \[astro-ph.CO\]](#).
- [48] N. Bernal, L. Necib, and T. R. Slatyer(2016), [arXiv:1606.00433 \[astro-ph.CO\]](#).
- [49] Y.-Y. Mao, L. E. Strigari, R. H. Wechsler, H.-Y. Wu, and O. Hahn, *Astrophys. J.* **764**, 35 (2013), [arXiv:1210.2721 \[astro-ph.CO\]](#).
- [50] D. McCammon *et al.*, *Astrophys. J.* **576**, 188 (2002), [arXiv:astro-ph/0205012 \[astro-ph\]](#).
- [51] A. Boyarsky, J. W. den Herder, A. Neronov, and O. Ruchayskiy, *Astropart. Phys.* **28**, 303 (2007), [arXiv:astro-ph/0612219 \[astro-ph\]](#).
- [52] S. G. Crowder *et al.*, *Astrophys. J.* **758**, 143 (2012), [arXiv:1209.1657 \[astro-ph.HE\]](#).
- [53] M. Ajello *et al.*, *Astrophys. J.* **689**, 666 (2008), [arXiv:0808.3377 \[astro-ph\]](#).
- [54] R. C. Hickox and M. Markevitch, *Astrophys. J.* **645**, 95 (2006), [arXiv:astro-ph/0512542 \[astro-ph\]](#).